Geophys. J. Int. (1990) **103**, 621–637

Deep seismic sounding studies in the north Cambay and Sanchor basins, India

K. L. Kaila, H. C. Tewari, V. G. Krishna, M. M. Dixit, D. Sarkar and M. S. Reddy
National Geophysical Research Institute, Hyderabad 500007, India

Accepted 1990 June 26. Received 1990 June 18; in original form 1989 December 6

SUMMARY

Deep seismic sounding (DSS) studies have been carried out in the north Cambay and Sanchor sedimentary basins in western India along three lines covering about 350 km. Seismic refraction and wide angle reflection data, pertinent to the sedimentary basin as well as the deep crustal section, have been recorded from 41 shot points using a 60 channel DFS-V digital recording system with 200 m geophone spacing and 4 ms data sampling. Extensive modelling and interpretation of a large number of seismic record sections reveal four sub-basins in the sedimentary section along these lines. Maximum depth to the granitic/Proterozoic basement (*P*-wave velocity 5.9–6.0 km s^{-1}) is about 5000 m in the north Sanchor and the Patan sub-basins and about 5600 m in the south Sanchor sub-basin. The deepest part of the sedimentary basin is delineated within the Gandhinagar sub-basin where the basement depth reaches 7700 m. The Deccan Traps (*P*-wave velocity 4.3–4.8 km s^{-1}) form the base of the Tertiary sediments, almost in the entire study area except the extreme northern part. There is also some indication of the presence of sub-Trappean Mesozoic sediments along this profile. Within the sedimentary basin two horst features, one near Diyodar (the Diyodar ridge) and the other northwest of Mehsana (the Unhawa ridge), are indicated by the seismic data consistent with the tectonics of the region.

The thickness of the upper crust in this region does not exceed 15 km (*P*-wave velocity reaching 6.3 km s^{-1}). A prominent low-velocity zone (velocity 5.5 km s^{-1}) occurs in the depth range from 10.5 to 12.5 km. The lower crust consists of two layers of velocities 6.6–6.9 km s^{-1} and 7.3–7.4 km s^{-1}, the discontinuity between them occurring at 23–25 km depth. The Moho discontinuity (P_M velocity 8.0 km s^{-1}) lies at a depth of 31–33 km. The high-velocity (7.3–7.4 km s^{-1}) lower crustal layer represents underplating of the crust due to mantle upwelling and rifting with large-scale extrusion of the Deccan volcanics. The large thickness of the Tertiary sediments in the Cambay basin and a relatively thin crust in the region suggest further rifting during the Tertiary.

Key words: Cambay basin, Deccan Traps, lower crust, Moho depth, seismic sounding.

1 INTRODUCTION

The Cambay basin in western India is a narrow, NNW–SSE trending buried graben extending from Tharad south-southeast through the alluvial plains of Gujarat, the Gulf of Cambay and into the Arabian sea. The basin originated during the Mesozoic period during the northward movement of the Indian subcontinent after the breakup of Gondwanaland and subsidence occurred mainly during the Tertiary (Biswas 1987). Shallow seismic investigations have been carried out extensively in this region by the Oil and Natural Gas Commission (ONGC), India.

Results of previous DSS studies, carried out in the southern part of the Cambay basin, were published by Kaila, Krishna & Mall (1981). As a logical continuation of the earlier work, additional DSS studies were continued

during 1986–87 towards the northern part of the Cambay basin from Mehmadabad (22°50′N, 72°46′E) to Tharad (24°27′N, 71°37′E) and towards the Sanchor basin up to Dharimanna (25°11′N, 71°27′E). The objectives of these DSS studies were (a) to map the granitic basement in the north Cambay and Sanchor basins, and (b) to determine the crustal *P*-wave velocity structure, and possibly infer the process of basin development in this region.

In order to accomplish the above, seismic refraction and reflection studies were carried out along the following three lines (Fig. 1): (i) Dharimanna–Sanchor–Tharad–Diyodar–Vijwada (line 1), (ii) Tharad–Diyodar–Patan–Mehsana–Gandhinagar (line 2) and (iii) Sadra–Mehmadabad–Degam (line 3). In addition to the refraction data, wide-angle reflections from the deep crustal reflectors and the Moho were also recorded along line 2 in the central part of the study area. To integrate these studies with results of the Mehmadabad–Billimora DSS profile in the south (Kaila *et al.* 1981) some additional spreads were also recorded. These data were acquired from 41 shot points using a 60 channel DFS-V digital recording system with 200 m geophone spacing and 4 ms data sampling. This paper deals with the analysis and interpretation of seismic refraction and wide-angle reflection data recorded along the three lines.

2 GEOLOGY AND TECTONICS OF THE REGION

The Cambay basin is covered with a thick layer of Quaternary and Tertiary sediments. In the east, most of the exposures consist of lower Cretaceous, upper and middle Jurassic and Proterozoic sediments. Some exposures to the west consist of Miocene and middle Jurassic formations (Fig. 1). Due to the large-scale oil exploration programme of ONGC, the sedimentary geology of the Cambay basin from the Tertiary to the Recent deposits is well known (Biswas 1982, 1987). The Mesozoic geology in the Cambay basin is not so well known as no wells, except a few on the basin margin, have penetrated the basic extrusives known as the Deccan Traps and reached the Mesozoic sediments. The Deccan Traps, which extruded around 67–68 Ma (Duncan & Pyle 1988), are considered to be the basement of the Tertiary sediments.

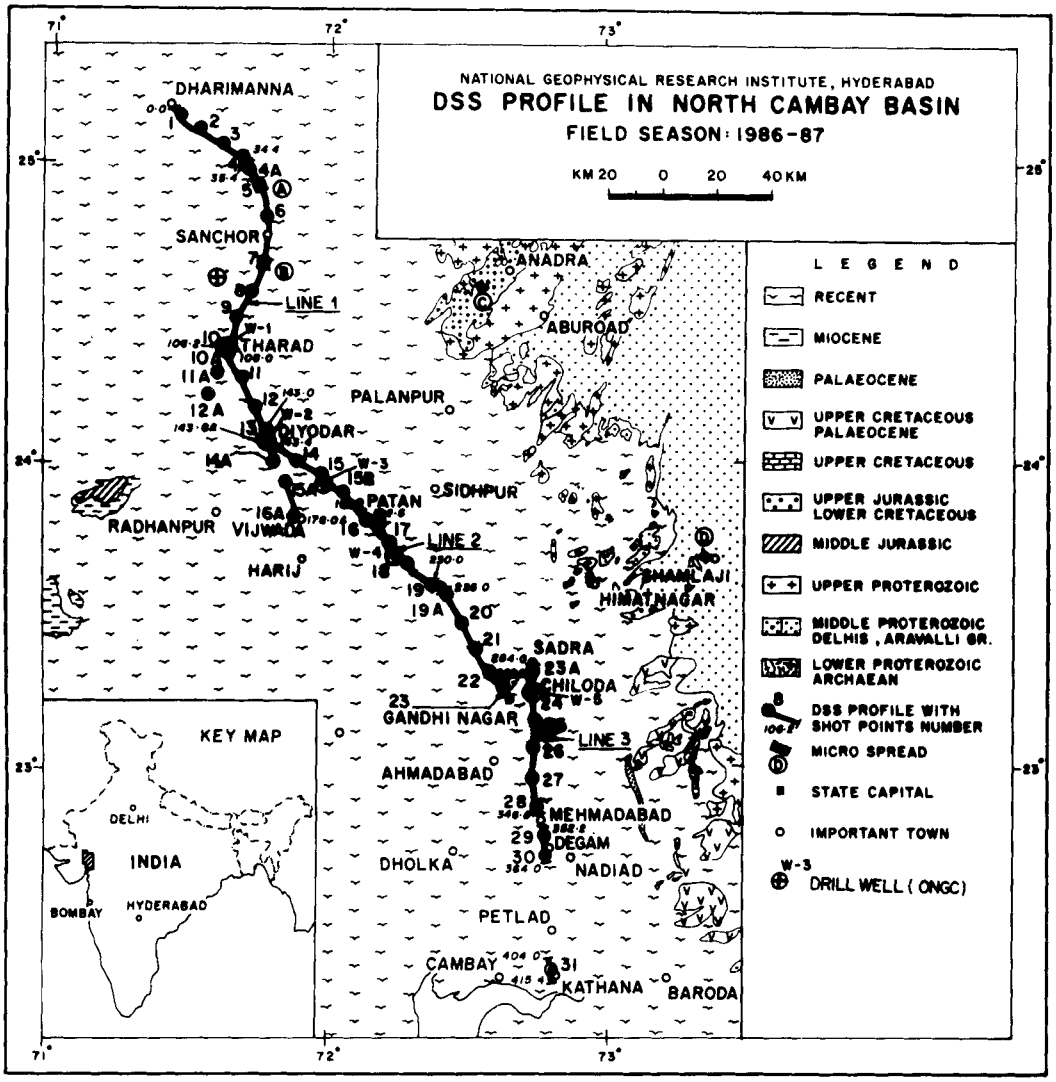

Figure 1. Locations of Lines 1, 2 and 3, along which the DSS studies were carried out in the north Cambay and Sanchor basins on the geological map of the region (after GSI 1962). Locations of some of the existing oil wells close to these lines are also shown.

Three pericontinental rift basins including the Cambay basin exist in the western margin platform of the Indian craton. These basins originated between the early Jurassic and Tertiary, during several stages of India's northward drift, after the breakup of Gondwanaland (Biswas 1982). They are bounded by intersecting sets of faults whose trends follow the three main Precambrian orogenic trends (Fig. 2) that represent the major orogenic cycles in western India: the Narmada–Son lineament along the ENE–WSW trend is a major tectonic boundary (West 1962; Choubey 1971) and divides the Indian shield into a southern peninsular block and a northern foreland block. The NE–SW Aravalli/Delhi trend spreads into three components; the main Aravalli trend continues across the Cambay basin while the Delhi trend swings E–W, producing a series of step faults. The third trend (NNW–SSE) swings eastwards and merges with the ENE–WSW Precambrian orogenic trend (Biswas & Deshpande 1983).

The Cambay basin was formed due to the extension in a northwest direction, of the NNW–SSE trend parallel to the west coast of India, into the western part of the Indian shield. The basin originated during the Mesozoic period but subsided at a greater rate during the Tertiary. It is flanked by the Aravalli swell comprising igneous and metamorphic rocks of Precambrian age in the northeast and the Deccan Traps in the east and west. The Deccan Traps represent the episode of volcanism marking the close of the Mesozoic era. On the east and west the basin is bounded by step faults (Fig. 3) which are not continuous in nature (Raju & Srinivasan 1983).

A large amount of geophysical information, concerning gravity-magnetic and seismic data, is available within the Cambay basin, this being one of the prominent oil bearing sedimentary basins in India. The Bouguer anomaly values in the basin (Fig. 4) are either comparable to or higher than those in the surrounding areas despite the presence of large sedimentary thickness within the basin. Based on the geophysical data and the available deep drilling results, Raju & Srinivasan (1983) have presented comprehensive models of various structural features within the basin that indicate basin formation, due to the rifting along the west coast of India as a sequel of sea-floor spreading, and its dissection into various units due to subsequent reactivation.

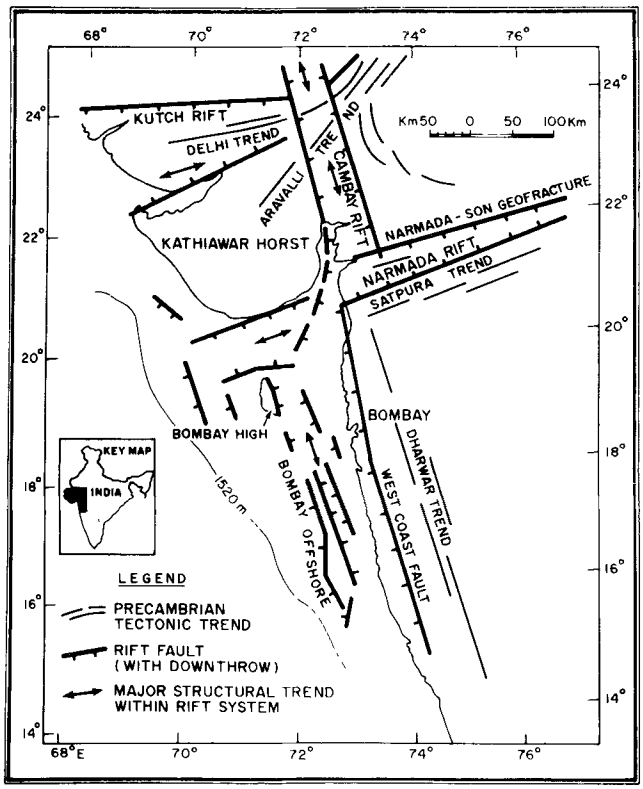

Figure 2. Tectonic map of the western India (after Biswas 1982).

3 PHASE IDENTIFICATION AND DATA INTERPRETATION

A total of 2844 line kilometres of traveltime data were recorded along the three lines from 41 shot points. Due to the close geophone spacing, various phases of first arrival refraction and wide-angle reflections could be identified on the seismograms. The interpretation of the sedimentary section up to the basement is based mainly on the first arrival refraction data (Fig. 5). Three velocities in the first arrivals, 2.1–2.2, 3.1–3.3 and 5.8–6.0 km s^{-1}, could be identified on most of the traveltime sections. Another velocity, of 4.3–4.8 km s^{-1}, however, could not be identified in all the first arrivals. In such cases it was derived by modelling the later arrival wide-angle reflections ($P^{4.5}$ in Fig. 6, $P^{4.8}$ in Fig. 7). Most of the basement faults could easily be identified on the basis of the sudden shift of the first arrival traveltimes in the updip direction (Figs 5 and 8). Towards the downdip direction relatively lower velocities were observed near the faults. The first arrival refraction traveltimes were inverted to give a velocity–depth section using the delay time approach and successive iteration of the model (Scott, Tibbvetti & Burdick 1972). Further modification of these depth sections was carried out by the ray tracing technique (Červený & Pšenčík 1981, 1983) to match the later arrivals (Figs 6, 7 and 9). The faults were replaced by high dips for the purpose of ray tracing. Oil well drilling results, wherever available, were also used to constrain the model (Fig. 10) particularly with respect to the presence of the Deccan Traps and the underlying Mesozoic sediments.

To define the sub-basement crustal model wide-angle reflections have primarily been relied upon. Four phases could be identified in the wide-angle reflections. Two phases from the upper crust ($P^{5.5}$, $P^{6.6}$) were identified as reflections (Figs 6, 7, 11 and 12) from the top and bottom of a low-velocity zone (LVZ), another phase ($P^{7.2}$) was recognized as the reflection from a high-velocity layer in the lower crust and the last phase ($P^{8.0}$) as the reflection from Moho (Figs 13, 14 and 15). Head waves of very weak amplitude from the Moho discontinuity could also be identified from one shot point (Fig. 14). Forward modelling by a ray tracing technique (Červený and Pšenčík 1981) was used to derive the crustal model (Fig. 16).

4 SEDIMENTARY BASIN STRUCTURE AND BASEMENT CONFIGURATION

For the purpose of shallow refraction studies, the data along each of the lines have been treated independently for interpretation. Fig. 10 represents the basement configuration along different lines of the profile compiled mainly from the data of Fig. 5. Since it is not possible to present all the data in this paper, some representative record sections of

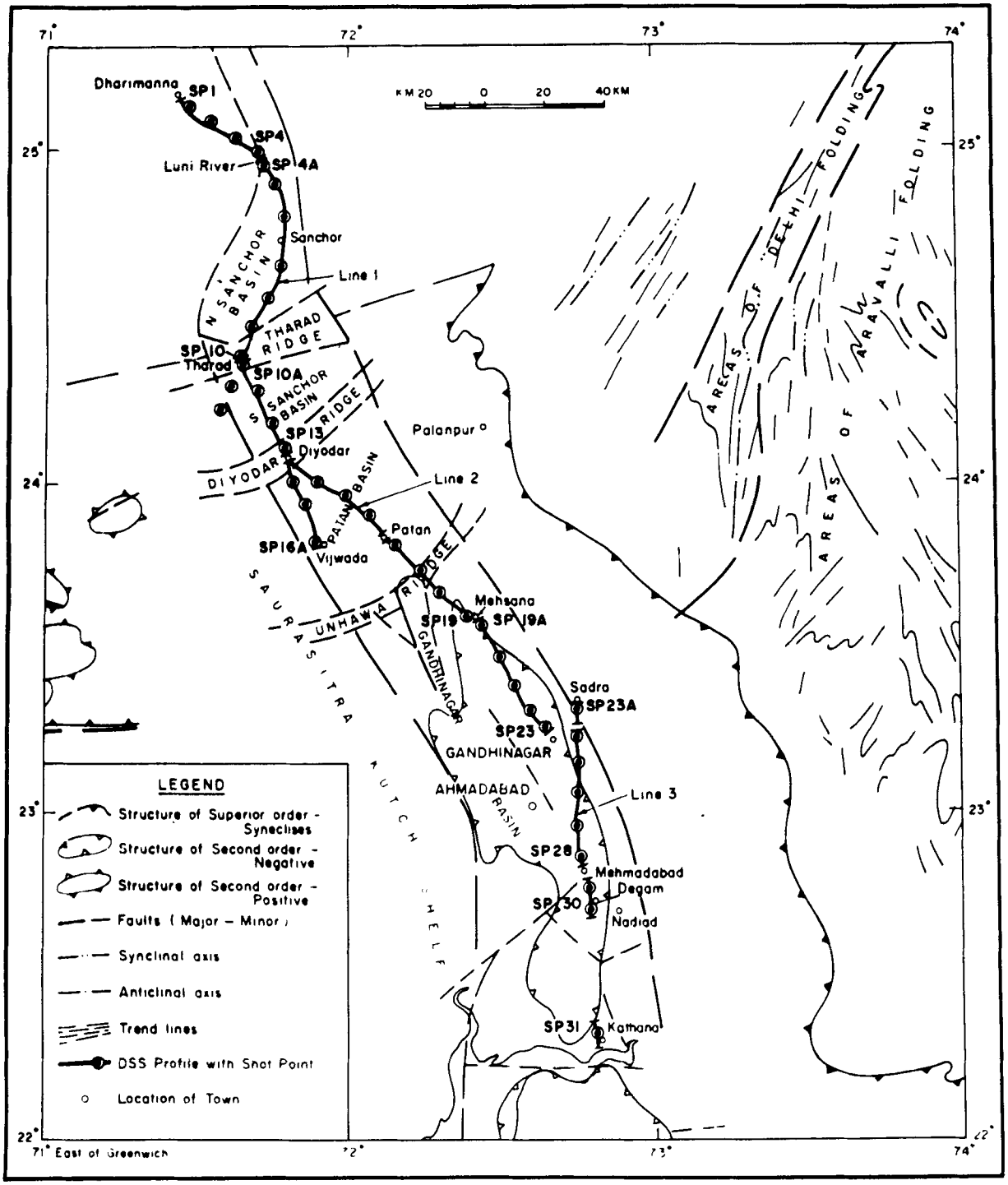

Figure 3. Detailed tectonic map of the north Cambay basin (after Raju & Srinivasan 1983). Lines 1, 2 and 3 are also shown.

the observed and synthetic seismograms plotted by trace normalization and the ray diagrams are shown in Figs 6, 7, 9, 11 and 12.

4.1 Line 1 (Dharimanna–Sanchor–Tharad–Diyodar–Vijwada profile)

This profile is further subdivided into three nearly straight line segments for studying the basement configuration.

4.1.1 Line 1A (Dharimanna–Luni river)

First arrival data from shot points (SPs) 1, 2, 3 and 4 (Fig. 5) have been used on this section. The computed depth section (Fig. 10) indicates a two-layer model in this region. The first layer of velocity 2.1 km s^{-1} is underlain by the basement layer of velocity 6.0 km s^{-1}. Near SP 1 the thickness of the sedimentary section is only about 350 m which increases gradually to about 1000 m near Luni river.

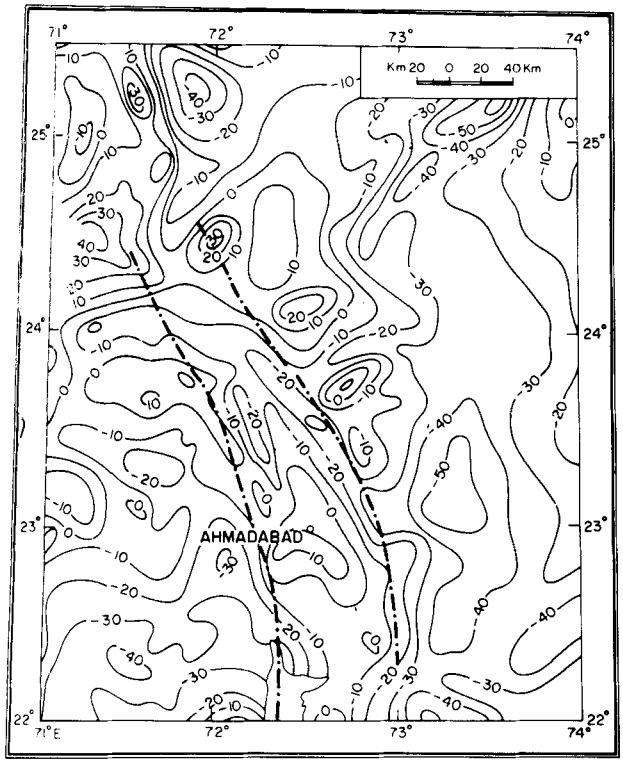

Figure 4. Gravity map of the Cambay region (after NGRI 1978). Boundaries of the Cambay basin (after Raju & Srinivasan 1983) are also shown by broken lines.

4.1.2 *Line 1B (Luni river–Sanchor–Tharad)*

First arrival data from SPs 4A, 5, 6, 7, 8, 9, 10, 11A and 12A (Fig. 5) have been used on this section. There is a recording gap between SP 4 and SP 4A. The sedimentary thickness seems to increase considerably to about 2900 m at SP 4A as compared to 1000 m at SP 4. The large change in the sedimentary thickness within a short distance of 3–4 km and the appearance of a new velocity layer (3.2 km s^{-1}) with thickness varying between 1000 and 3000 m towards south of SP 4A indicates either a steep dip or a possible fault between SP 4 and SP 4A. We prefer to interpret it as a fault (Fault F1, Fig. 10) which may correspond to the location of the Luni river. The layer of velocity 3.2 km s^{-1} directly overlies the basement (velocity 5.9–6.0 km s^{-1}) between SP 4A and SP 7. However, a new layer of velocity 4.5 km s^{-1} is present towards the south of SP 7. By a comparison with the drilling data available from a deep well near SP 10 this layer is inferred to be the Deccan Traps. Two deep wells in this area (Fig. 1), one very near to the profile and another on the fringes of the basin (not shown in Fig. 10), show the Traps thickness of 475–490 m underlain by the Mesozoic sediments (Fig. 10). Based on this evidence, the Deccan Traps layer has been modelled with an average thickness of 500 m followed by a layer of the Mesozoic sediments of velocity 3.9 km s^{-1}. The maximum depth to the basement in this model is about 5000 m below SP 9. If the Mesozoics are not considered, the maximum depth to the basement could, however, be about 5800 m between SP 9 and SP 10.

4.1.3 *Line 1C (Tharad–Diyodar–Vijwada)*

First arrival data from SPs 10A, 11, 12, 13, 14, 14A, 15A and 16A (Fig. 5) have been used for this part of the section (Fig. 5). Between SP 10A and SP 13 a four-layer model, which appears to be the continuation of the model along Line 1, has been inferred (Fig. 10). This four-layer section terminates near SP 13 against a steep updip and/or a fault. The basement (velocity 6.0 km s^{-1}) is at a depth of 5000 m between SP 11 and SP 12. It appears to rise to a shallow depth of less than 2000 m below SP 13 due to the fault F2. The layer of velocity 4.3 km s^{-1} is likely to be the continuation of the Deccan Traps inferred around SP 10 at a depth of 1700 m. It is not possible to conclusively show the presence of the Mesozoics under this layer in the absence of any drilling data. However, the thickness of the 4.3 km s^{-1} velocity layer is about 3000 m and it is likely to represent a combination similar to that north of SP 10. This configuration is likely to continue till SP 13.

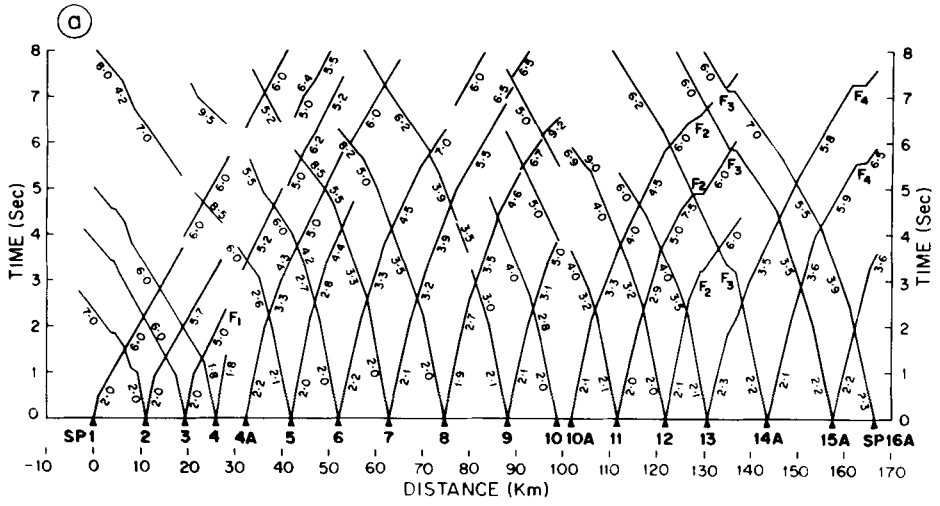

Figure 5. First arrival refraction traveltime data used for preparing the depth section up to the basement along (a) Line 1, (b) Line 2 and (c) Line 3. Apparent velocities of the first arrivals and the interpreted fault locations are also shown.

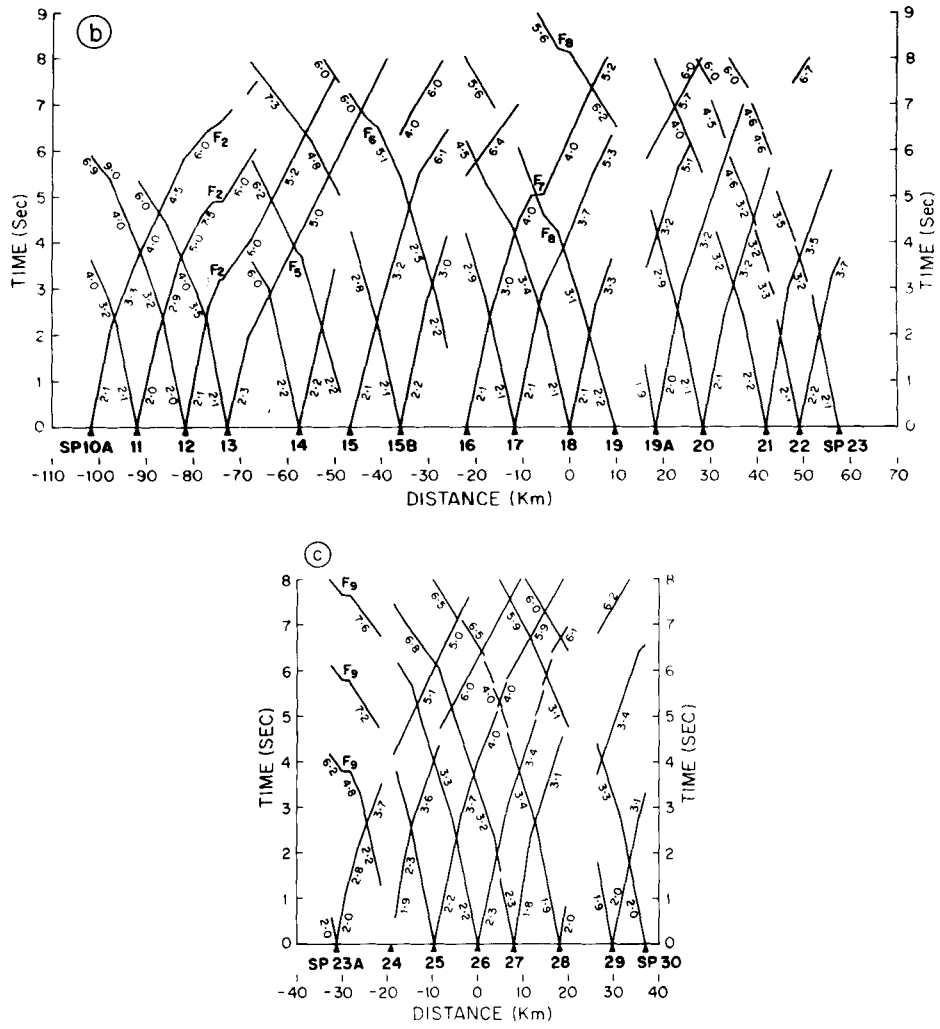

Figure 5. (*continued*)

South of SP 13, a four-layer model is conceived, the velocities in the layers being 2.1, 3.2, 4.5 and 5.9 km s^{-1}. The 4.5 km s^{-1} velocity layer, which could not be recognized in the first arrivals, has been identified in the later arrivals and by correlation with the well data. Maximum depth to the basement (velocity 5.9 km s^{-1}) in this part is about 5000 m between SP 14A and SP 15A. Due to the basement fault near SP 16A, this depth reduces to about 1300 m towards the south of the fault F4. The region between SP 13 and SP 14A is a basement uplift, bounded by the fault F3 towards the south and a steep updip/fault (F2) towards the north. Basement depth in this part is 1500–2000 m. The faults F2, F3 and F4 showing large changes in the sedimentary thickness are identified on the basis of shifts in the first arrival traveltimes (Figs 5 and 8). A deep well near SP 13 (Fig. 1) has yielded a sedimentary thickness of 1650 m followed by the Deccan Traps. Drilling of this well has been terminated in the Traps at a depth of 1950 m (Fig. 10).

4.2 Line 2 (Tharad–Gandhinagar profile)

This profile is an extension of Line 1C from SP 13 in the NW–SE direction and has been divided into two sections, towards the north and south of Mehsana, for convenience of interpretation.

4.2.1 *Line 2A (Diyodar–Patan–Mehsana)*

First arrival data from SPs 13, 14, 15, 15B, 16, 17, 18 and 19 (Fig. 5) have been analysed on this section. The layer configuration near SP 13 is similar to the model along Line 1C between SP 13 and SP 14A. Beyond that a four-layer configuration is inferred with velocities of 2.1, 3.2, 4.5 and 5.9 km s^{-1} (Fig. 10). Maximum depth to the basement is about 6000 m between SP 15 and SP 16. In the horst region between SP 17 and SP 18 bounded by faults F7 and F8 which were recognized on the basis of clear shifts in the first arrival traveltimes (Figs 5 and 8), the basement is at a depth of 2200 m. Towards the southeast of this horst, the basement depth increases to 6200 m under SP 19.

In the drilled oil wells in the region of SPs 17–19 (Fig. 1) the Deccan Traps have been encountered at depths varying from 1600 to 2050 m (Fig. 10). In another well near SP 15 (Fig. 1), Trap derivatives have been encountered at a depth of about 3000 m (Fig. 10). Based on these well data and the observations of wide-angle reflections in the later arrivals ($P^{4.5}$, Fig. 6) the layer of velocity 4.5 km s^{-1}, which could

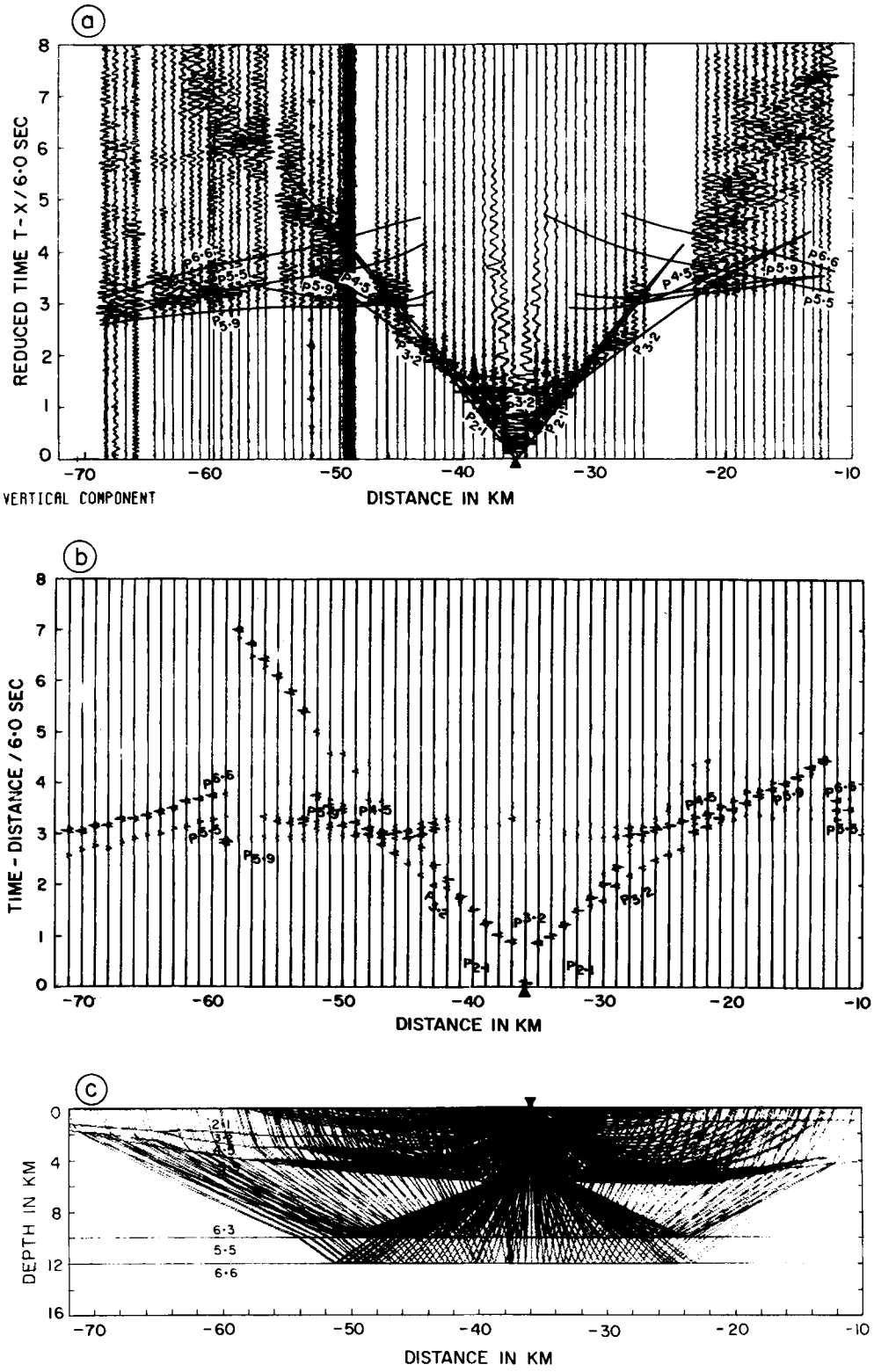

Figure 6. Record section of (a) observed (b) ray synthetic seismograms and (c) ray diagram with velocity model, for SP 15B (shown by triangles). Traveltime curves for various phases, are marked by P_k (refractions) and P^k (reflections) for the model shown in Fig. 10 (Line 2). k represents the layer velocity in km s^{-1}. In (a) the hidden layer is seen as later arrival reflections ($P^{4.5}$) at −52 to −45 and −32 to −16 km. Reflections from top and bottom of the LVZ ($P^{5.5}$, $P^{6.6}$) can be seen at −70 to −55 and −70 to −60 km respectively.

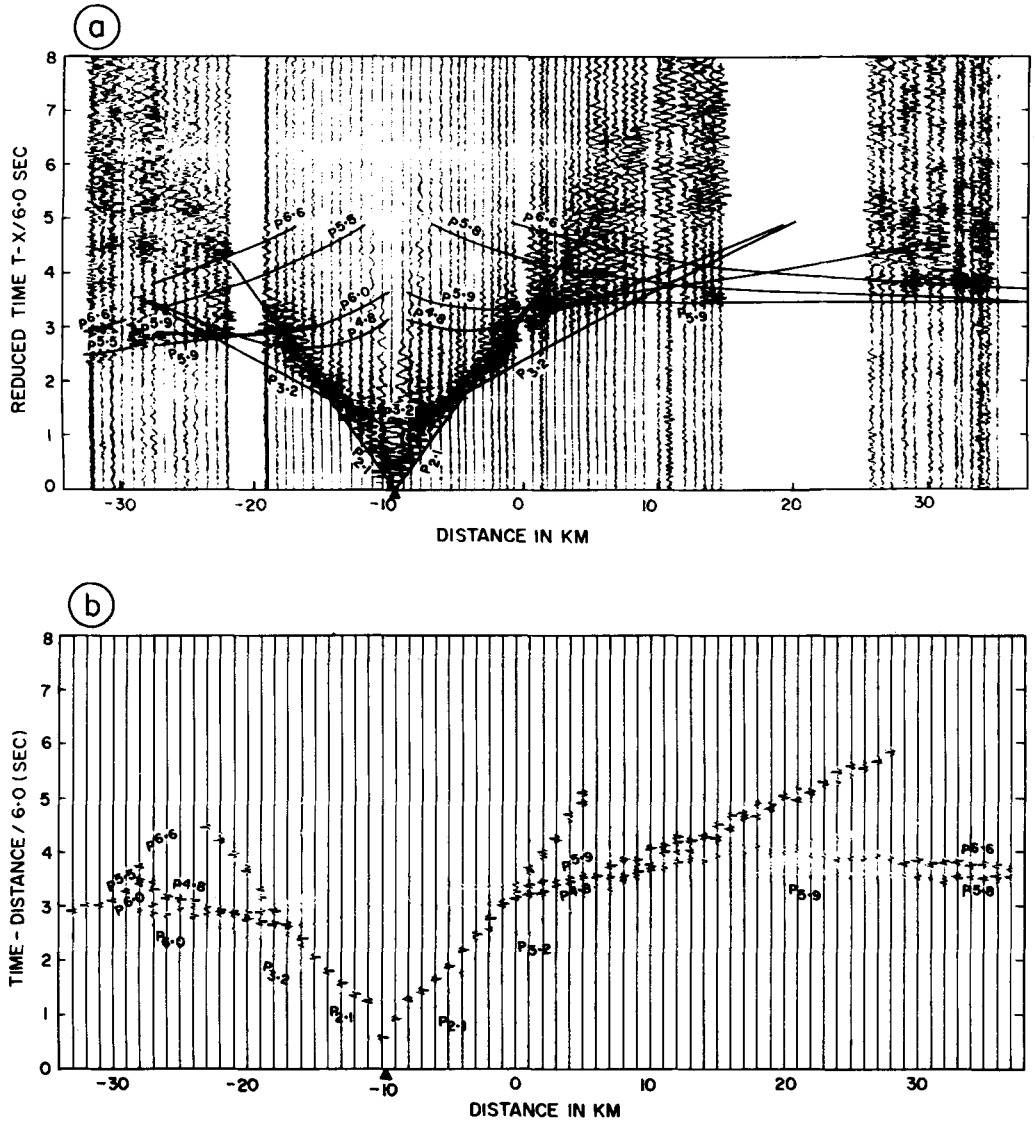

Figure 7. Record section of (a) observed and (b) ray synthetic seismograms for SP 25 (shown by triangles) for the model shown in Fig. 10 (Line 3). Symbols used for various phases are same as in Fig. 6. In (a) the hidden layer is seen as later arrival reflection ($P^{4.8}$) at −2 to 10 km. Reflections from top and bottom of the LVZ ($P^{5.8}$, $P^{6.6}$) are seen at 26–35 km.

not be observed in the first arrivals, has been interpreted as the Deccan Traps layer. It is not possible to infer the presence or otherwise of the Mesozoic sediments under the Traps layer due to the absence of any other information especially from drilled wells. However, as the Traps layer is not very thick, the chances of the Mesozoics being present below are very small.

4.2.2 Line 2b (Mehsana–Gandhinagar)

First arrival data from SPs 19A, 20, 21, 22 and 23 (Fig. 5) have been used on this section. A four-layer model (Fig. 10) has been inferred, the velocities in the four layers being 2.1, 3.1, 4.5 and 6.0 km s^{-1}. The layer of velocity 6.0 km s^{-1} is at a depth of about 6200 m below SP 19A. This depth increases to a maximum of 7700 m near SP 22. The wells in this region have not reached such depths to indicate the nature of the 4.5 km s^{-1} velocity layer. However, a model consistent with the interpretation along Line 2a suggests that this layer may also correspond to the Deccan Traps. In the absence of observable reflections from the top and bottom of a velocity reversal, it is not possible to conclusively show the presence or absence of the Mesozoic sediments of lower velocity below the inferred Traps layer of relatively high velocity. However, as the inferred thickness of the Traps layer is more than 2000 m, it is likely that a part of this section may consist of the Mesozoic sediments beneath the Traps. The layer of velocity 6.0 km s^{-1} represents the basement in this region.

4.3 Line 3 (Sadra–Mehmadabad–Degam profile)

First arrival data from SPs 23A, 24, 25, 26, 27, 28, 29 and 30 (Fig. 5) have been used on this section. This profile is

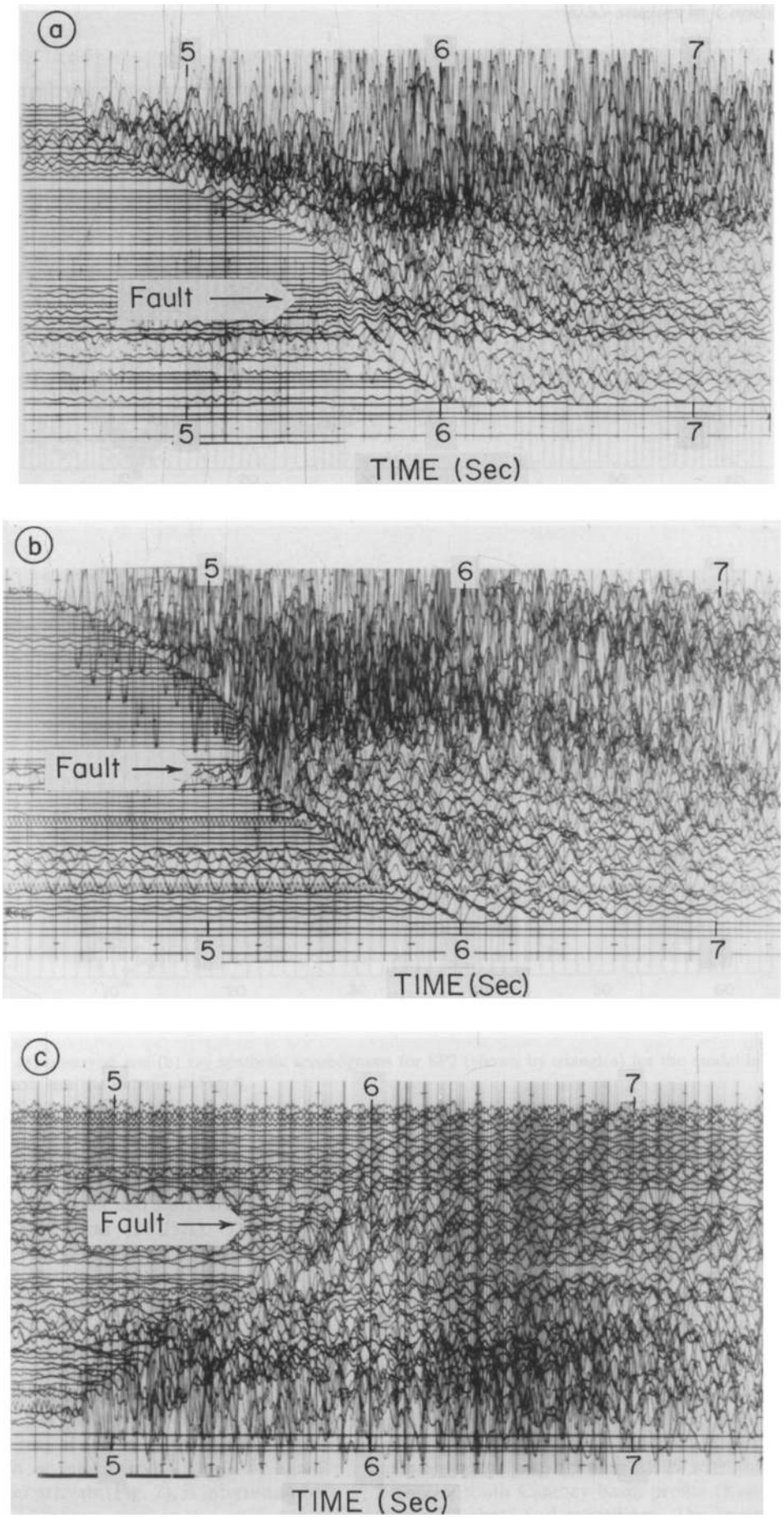

Figure 8. Sample field records from (a) SP 14A on Line 1 (b) SP 16 on Line 2 and (c) SP 25 on Line 3 showing shifts of first arrivals in the updip directions which have been inferred as faults F4, F7 and F9 respectively.

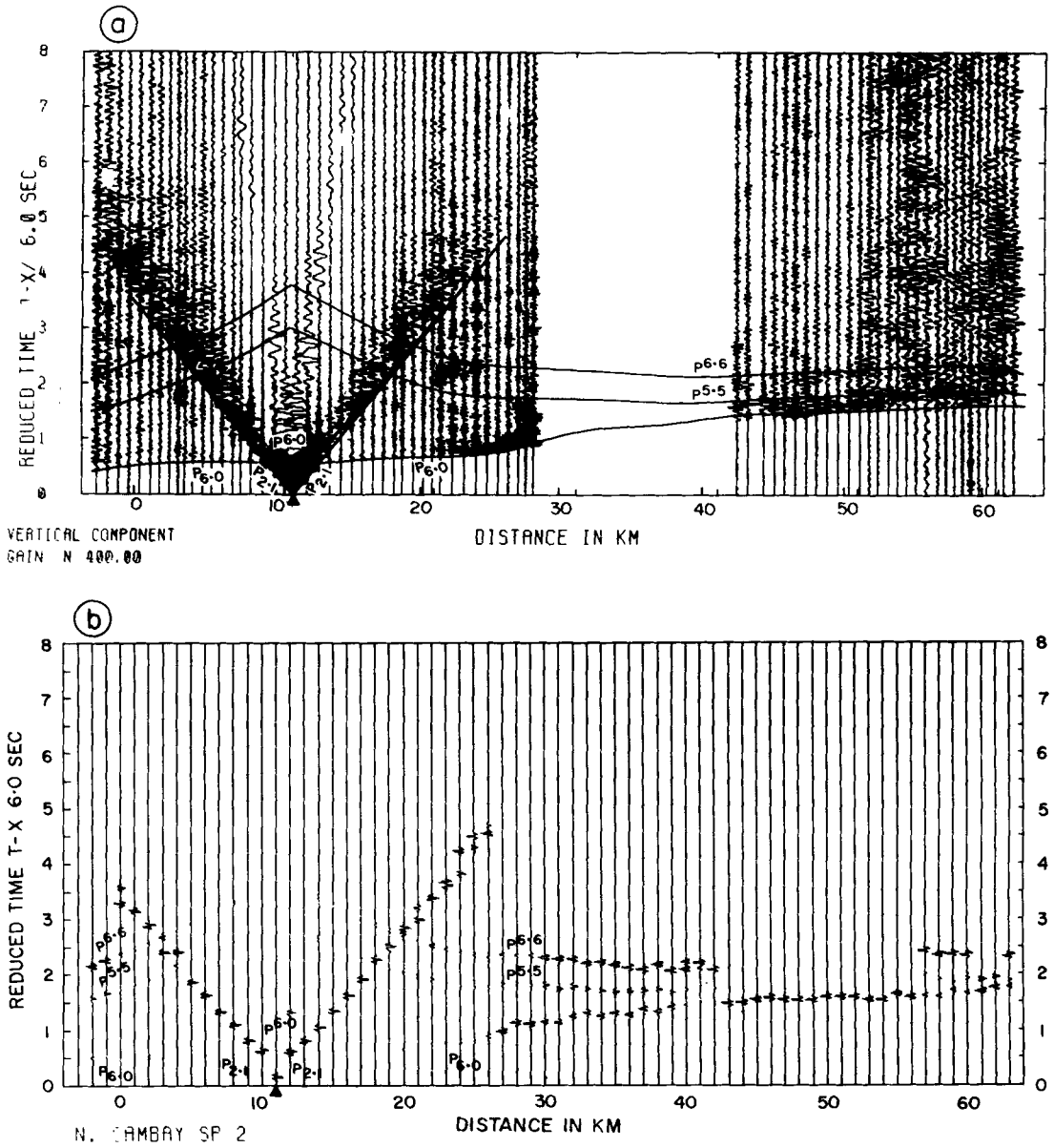

Figure 9. Record section of (a) observed and (b) ray synthetic seismograms for SP2 (shown by triangles) for the model in Fig. 10 (Line 1a). Symbols used for various phases are the same as in Fig. 6.

approximately in the N–S direction and starts from outside the Cambay graben in the north (SP 23A). The depth section along this profile (Fig. 10) reveals a four-layer model with velocities of 2.1–2.2, 3.1–3.3, 4.8 and 5.9–6.0 km s^{-1} respectively. The basement (velocity 5.9–6.0 km s^{-1}) is at a depth of about 200 m below SP 23A. Due to faulting (Figs 5 and 8) and steep downdip it attains a depth of about 5500 m below SP 24. This depth increases to 6900 m below SP 26, which is maintained up to SP 30. A deep well about 5 km north of SP 24 (Fig. 1) has shown the presence of the Deccan Traps at a depth of about 2700 m (Fig. 10). Therefore the layer with a velocity of 4.8 km s^{-1}, again recognized only in the later arrivals (Fig. 7), is inferred to be the Deccan Traps layer.

5 DEEP CRUSTAL STRUCTURE

The deep crustal model of the north Cambay basin has been delineated in the central portion of the study area by forward modelling of seismic refraction and wide-angle reflection data with the aid of the software packages SEIS81 and SEIS83 (Červený & Pšenčík 1981, 1983). North of SP 10 only upper crustal structure could be derived as the data acquisition was limited to 40–50 km recording distance from each shot point. Long distance data from the lower crust and the Moho were recorded along Lines 2 and 3, including some overlap near SP 29 with the Mehmadabad–Billimora south Cambay basin profile (Kaila *et al.* 1981) by additional shots and recordings. The crustal models along

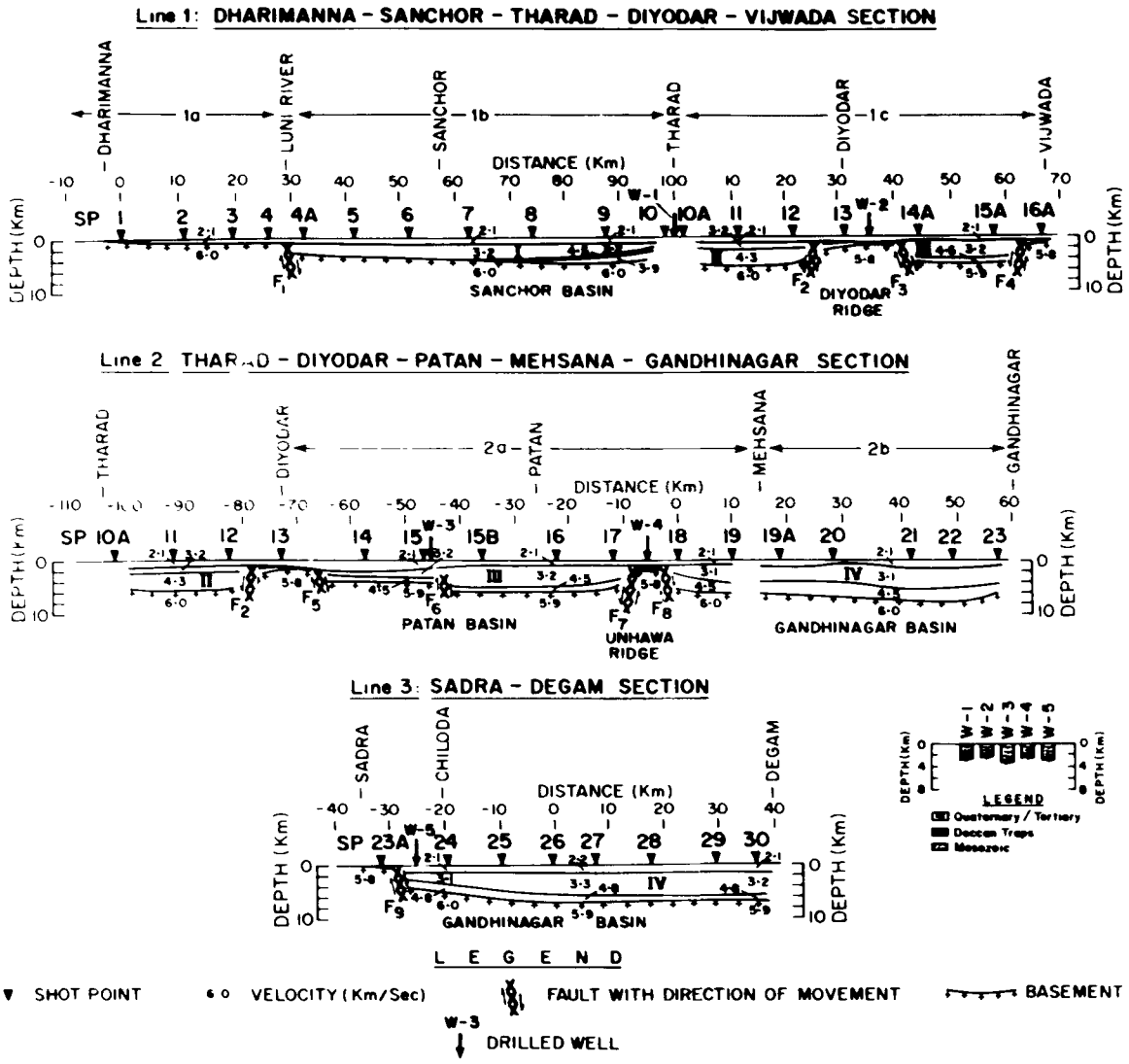

Figure 10. Basement configuration along Lines 1, 2 and 3 showing various sub-basins and basement ridges.

Line 1 and along Lines 2 and 3 (Fig. 16) will be discussed separately.

5.1 Line 1 (Dharimanna–Tharad section)

This section falls mainly in the Sanchor basin which is connected to the northern end of the Cambay basin. The upper crustal structure of the Sanchor basin has been obtained to a depth of 15 km with the help of the data from SPs 2 (Fig. 9), 4, 4A, 5, 6 (Fig. 11), 7 and 10. In this paper we show some illustrative seismograms for SPs 2 and 6 in Figs 9 and 11 respectively. In the trace normalized field records of most of these shot points two prominent events appear at 35–50 km distance from the respective shot points (Fig. 11). These two events are almost parallel to each other and appear at about the same distance range. Their relative amplitudes are much higher compared to the first arrivals. These properties, possibly of the reflection phases, suggest that a low-velocity zone (LVZ) may exist, the two reflections ($P^{5.5}$, $P^{6.6}$) corresponding to the top and bottom of the LVZ, and the inferred velocity of 5.5 km s^{-1} in the LVZ is such that the synthetic amplitudes of the reflections are comparable with the observations. The large contrast between the velocity in the LVZ (5.5 km s^{-1}) with respect to the velocity at its top (6.2 km s^{-1}) is found necessary to produce the required relative amplitudes for these two reflections (Fig. 11). The thickness of this LVZ is about 2 km. Along the Line 1a, the top and bottom of the LVZ are at depths of 8 and 10 km respectively while along Line 1b this layer appears to be dipping towards the south with its top varying from 10.5 to 12.5 km and bottom 12.5 to 14.5 km depth. The mismatch of relative amplitudes from these layers towards the left of SP 6 could be due to the effect of fault F1 which probably effects these layers as well.

5.2 Lines 2 and 3 (Tharad–Degam section)

The deep crustal model in this region has been delineated mainly from the data of SPs 10A (Fig. 13), 14A, 18, 26, 29 (Fig. 14) and 31 (Fig. 15). Use has also been made of the record sections of intermediate shot points (Figs 6 and 7) to constrain the velocity structure in the upper crust. Forward

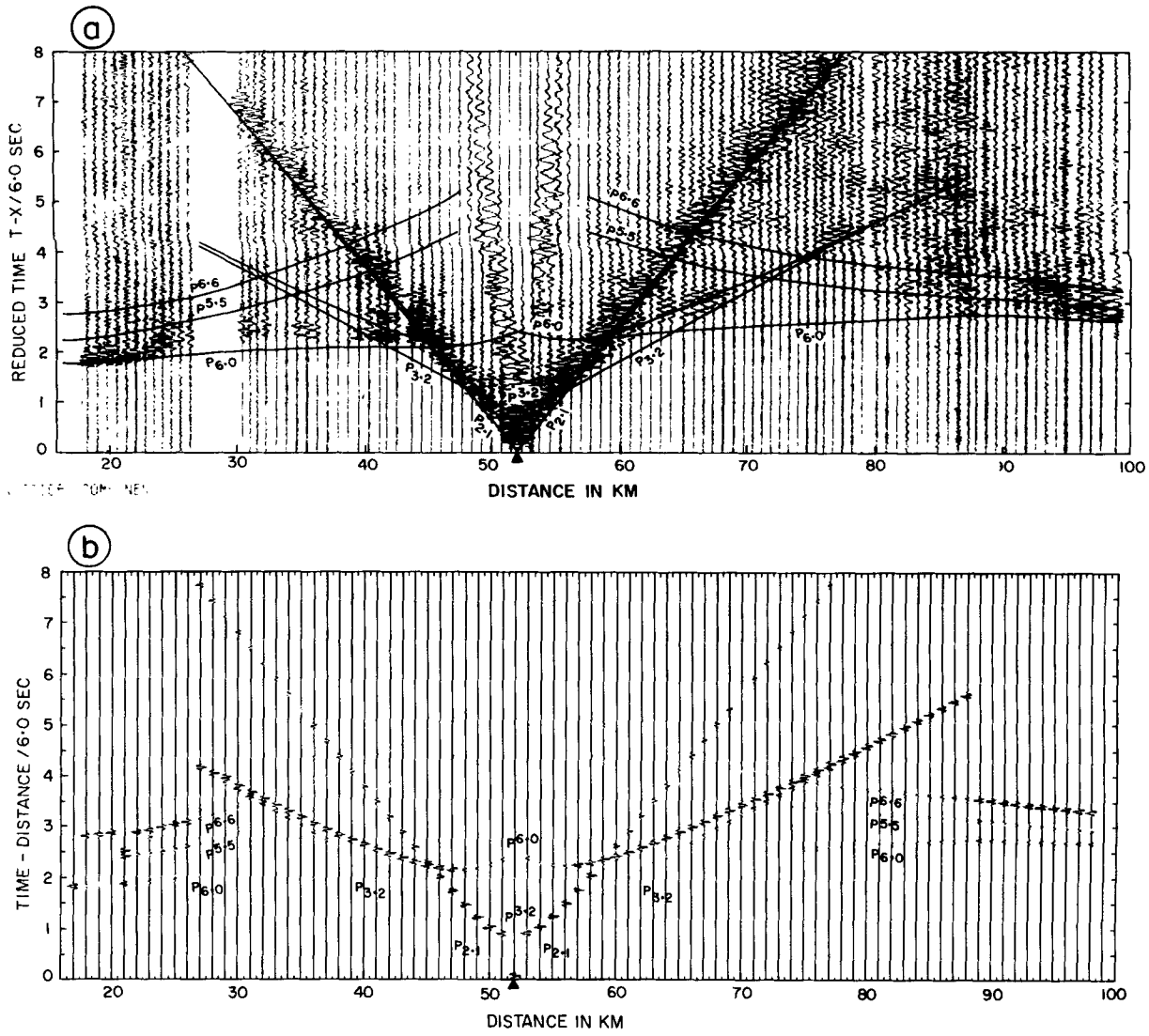

Figure 11. Record section of (a) observed and (b) ray synthetic seismograms for SP 6 (shown by triangles) calculated for the model shown in Fig. 10 (Line 1b). Symbols used for different phases are the same as in Fig. 6. In (a) the wide-angle reflections from the top and bottom of the LVZ shown in Fig. 16 ($P^{5.5}$, $P^{6.6}$) are seen at 85–100 km.

modelling of record sections has been carried out, for each shot point, after identifying the reciprocal reflection data. The results from all the shot points have been combined to infer the plausible earth model. The upper crustal LVZ of 5.5 km s^{-1} velocity appears to be present throughout the Cambay basin at depths between 10.5 and 12.5 km consistent with the section on Line 1. The velocity from the top of the basement to its base, above the LVZ, varies from 5.9–6.0 to 6.2–6.3 km s^{-1}. At the base of the LVZ the velocity increases from 5.5 to 6.6 km s^{-1} (Figs 6, 7 and 12).

The velocity increases from 6.6 km s^{-1} with a small gradient, till another velocity discontinuity is encountered at a depth of 23–25 km. At this discontinuity the velocity increases from 6.7–6.9 to 7.2–7.4 km s^{-1}. The reflections from this discontinuity ($P^{7.2}$) are strong at distances of 70–110 km from respective shot points, and generally weak at larger distances (Figs 13, 14 and 15). This discontinuity, also delineated by Kaila *et al.* (1981) in the southern profile, seems to be present throughout the Cambay basin. From this discontinuity down to the Moho, the velocity remains in the range of 7.2–7.4 km s^{-1} representing a zone of high velocity within the lower crust.

Another strong reflector ($P^{8.0}$) identified as the Moho, appears at recording distances beyond 70–80 km from the shot points 10A (Fig. 13), 14A, 18, 26, 29 (Fig. 14) and 31 (Fig. 15). A first-order velocity jump from 7.3–7.4 to 8.0–8.1 km s^{-1} has been inferred at the Moho depth by modelling. Synthetic amplitudes of reflections from the Moho with such a velocity jump satisfactorily match the observations on most of the field seismic records (Figs 13, 14 and 15). The depth to the Moho discontinuity is found to be 32–33 km along Line 2 and 31 km along the Line 3. Head waves from the Moho discontinuity ($P_{8.0}$), although of weak amplitude, have also been identified with an apparent velocity of 8.0 km s^{-1} on the record section from SP 29. Their amplitudes in Fig. 14 appear to be very small due to normalization with respect to relatively high amplitudes in the later arrivals.

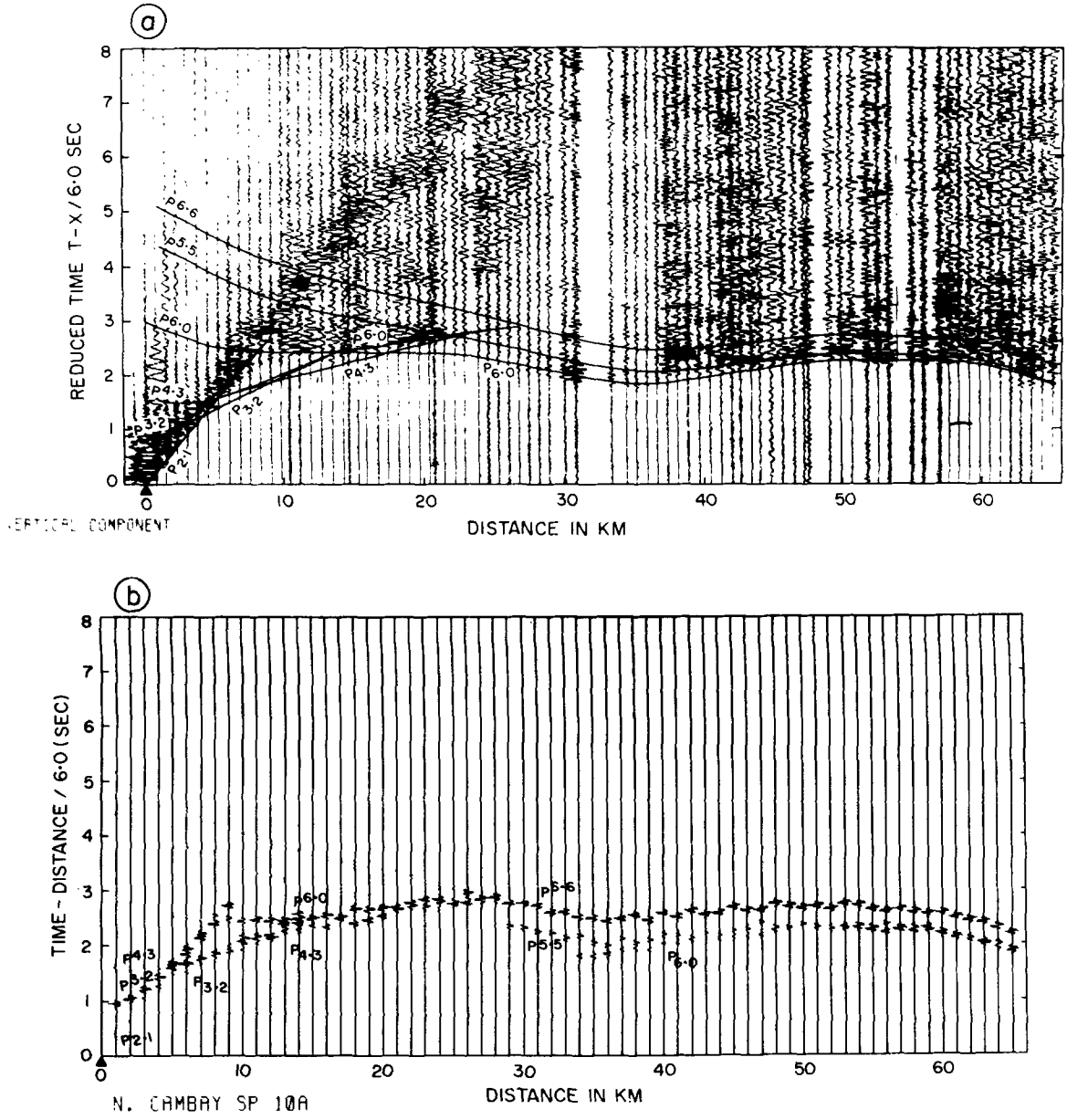

Figure 12. Record section of (a) observed and (b) ray synthetic seismograms from SP 10A (shown by triangles) for the model shown in Fig. 10 (Line 1c). Symbols used for various phases are the same as in Fig. 6. In (a) the wide-angle reflections from the top and bottom of the LVZ shown in Fig. 16 ($P^{5.5}$, $P^{6.6}$) are seen at 35–60 km. The decrease in traveltimes between 25 and 45 km is caused by the Diyodar ridge.

As can be seen from Fig. 13 (from 90 to 105 km) and 14 (from 85 to 95 km) and also from the corresponding synthetic seismograms, the later events are affected by variations in the thickness of the sedimentary section. The sudden changes in the traveltimes appearing as sharp bends consistently for first as well as later arrivals, as can be seen in Figs 13 and 14, are the statics due to the sudden reduction in the thickness of sediments between faults F7 and F8 (Fig. 16).

The crustal model of the north Cambay basin presented here compares quite well with the model given for the northern part of the Mehmadabad–Billimora profile by Kaila *et al.* (1981). In both the models, the Moho has been inferred at 31–32 km depth near Mehmadabad (SP 29, Fig. 1). The higher velocity lower crustal layer of velocity 7.3–7.4 km s^{-1} also compares quite well and is consistently present in both the profiles at depths of 20–25 km. However the upper crustal LVZ, shown in Fig. 16, has been brought out in the present study with the aid of relative amplitude modelling of the high-quality digital data in the north Cambay basin.

6 INTERPRETATION AND DISCUSSION OF THE RESULTS

Along the present DSS profile the basement (velocity 5.8–6.0 km s^{-1}) appears to be faulted at several places (Fig. 10). The fault F1 probably represents the western margin

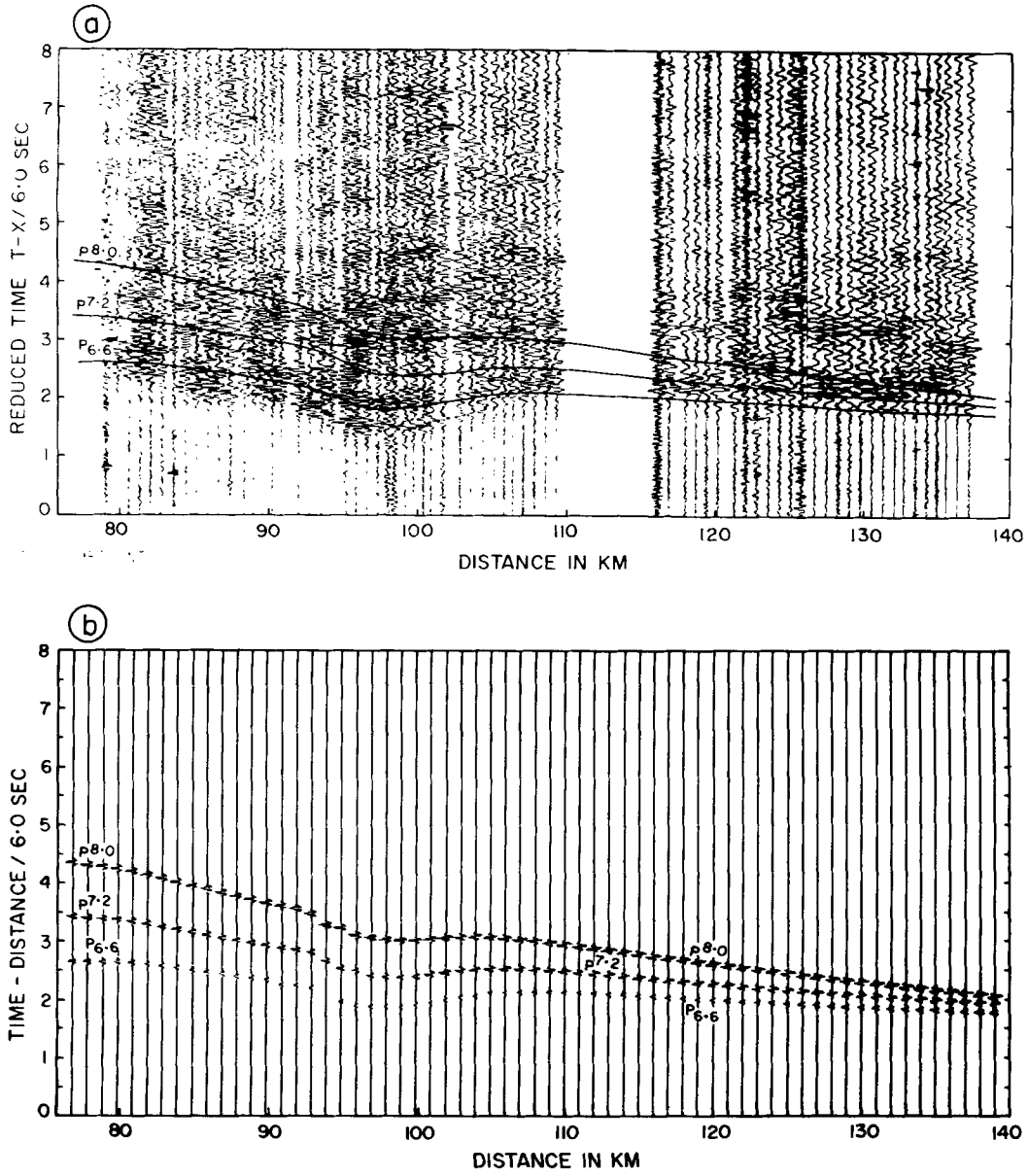

Figure 13. Record section of (a) observed and (b) ray synthetic seismograms on Line 2, for SP 10A. The shot point is located at 76 km distance from the left margin. Traveltime curves shown are calculated for various phases, for the model shown in Fig. 16. In (a) the wide-angle reflections ($P^{6.6}$, $P^{7.2}$ and $P^{8.0}$) can be seen at 80–100, 85–130 and 100–138 km respectively. The decrease in traveltimes between 90 and 105 km is caused by the Unhawa ridge.

fault of the north Sanchor basin, against which Tertiary sediments of this basin appear to terminate. A basement horst occurs near SP 13, with two bounding faults (F2 and F3), that separates the Sanchor basin to the north from the Patan basin to the south. On Line 2 another fault (F5) appears below SP 14. Both the faults F3 and F5 represent the southern culmination of the Diyodar ridge on two different profiles. The basement fault (F6) between SP 15 and SP 15B is responsible for the deeper part of the Patan basin. Another horst feature, bounded by the faults F7 and F8 between SP 17 and SP 18, has been inferred to correspond to the Unhawa ridge which crosses the Cambay basin (Fig. 3). The fault (F9), near SP 23A on the northern end of the Line 3, represents the eastern margin of the Cambay basin.

The results of this study show that the northern part of the Cambay graben contains a few horst structures which represent the structural trends across the basin. Four sub-basins have been identified in this region. The first one, the north Sanchor basin, starts south of the Luni river. The northern part of this sub-basin is either devoid of or has only a small thickness of the Deccan Traps and/or Mesozoics; while in its central part, up to the Tharad ridge, Traps/Mesozoics seem to be present. The second sub-basin which is separated from the first by a ridge structure near Tharad is possibly the southern continuation of the Sanchor

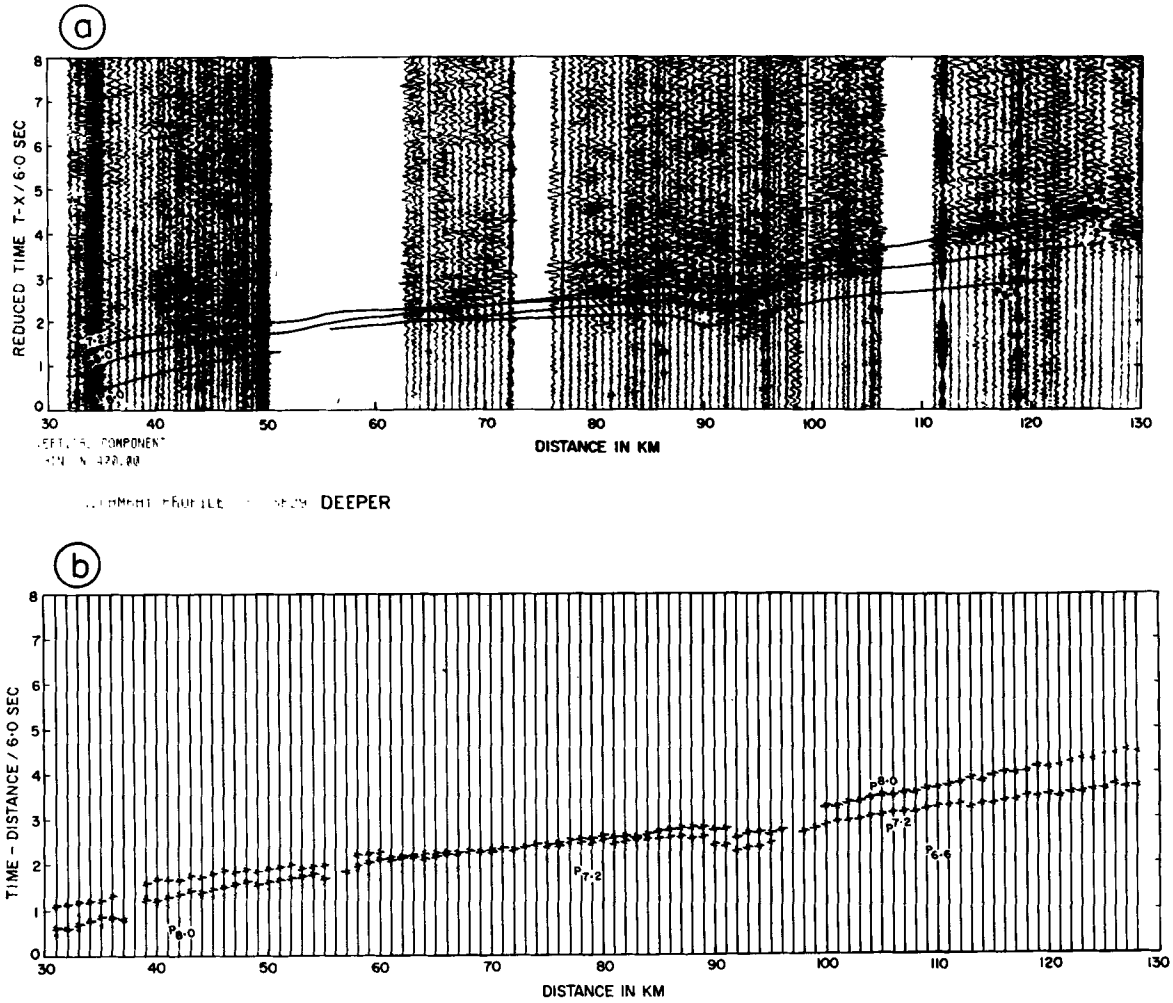

Figure 14. Record section of (a) observed and (b) ray synthetic seismograms on Line 2 for SP 29. The shot point is located at 81 km from the right margin. Traveltime curves shown are calculated for various phases, for the model shown in Fig. 16. In (a) the wide-angle reflections ($P^{7.2}$ and $P^{8.0}$) can be seen at 85–130 and 65–125 km respectively. The decrease in traveltimes between 85 and 100 km is caused by the Unhawa ridge.

basin and has a considerable thickness of the Traps/Mesozoics column. The Tharad ridge (Fig. 3) does not appear to be a well-developed basement ridge, and is more likely to represent a basement high within the Sanchor basin (Fig. 10). The third sub-basin, the Patan basin, is separated from the second one by the Diyodar ridge and continues up to the Unhawa ridge (between SP 17 and SP 18 on Line 2 and up to SP 16A on Line 1C) and appears to be mainly a Tertiary basin. Though the Traps appear to be present, there is little chance for the presence of Mesozoics beneath them. The fourth sub-basin, the Gandhinagar basin, extends towards south of Unhawa ridge and continues up to the end of the profile. The Deccan Traps/Mesozoics section seems to be present in this part.

It appears that the Mesozoic sediments are either absent or have only very little thickness in the Patan basin (Fig. 10) while on both sides of it the possibility of occurrence of these sediments beneath the Traps is fairly high. This suggests that the Patan basin was not formed during the Mesozoic period and instead the area was a plateau of Proterozoic sediments of the Delhi/Aravalli system. During Early Tertiary period, this area subsided, creating the Patan basin in which mainly the Tertiary/Quaternary deposition took place. The Diyodar and Unhawa ridges seem to be remnants of the Proterozoic plateau. This also means that the northern boundary of the Cambay basin during the Mesozoic period was limited by the Unhawa ridge.

The high-velocity lower crustal layer ($7.3\,km\,s^{-1}$), is present throughout the Cambay basin as shown by the present study as well as Kaila *et al.* (1981). This high velocity is, however, not found in the crust beneath the neighbouring Deccan Traps covered areas of Saurashtra to its west, across the Narmada lineament to its east (Kaila, Tewari & Sarma 1980; Kaila *et al.* 1989) and the Koyna region to its south (Krishna, Kaila & Reddy 1989). White & McKenzie (1989) argued that the presence of a high-velocity lower crustal layer in a rift zone and its absence in the adjacent areas is evidence that can be attributed with confidence to the igneous accretion. In their view, the intensive volcanism at the time of crustal extension and continental rifting resulted in the formation of the Deccan flood basalts and the concurrent igneous activity on offshore

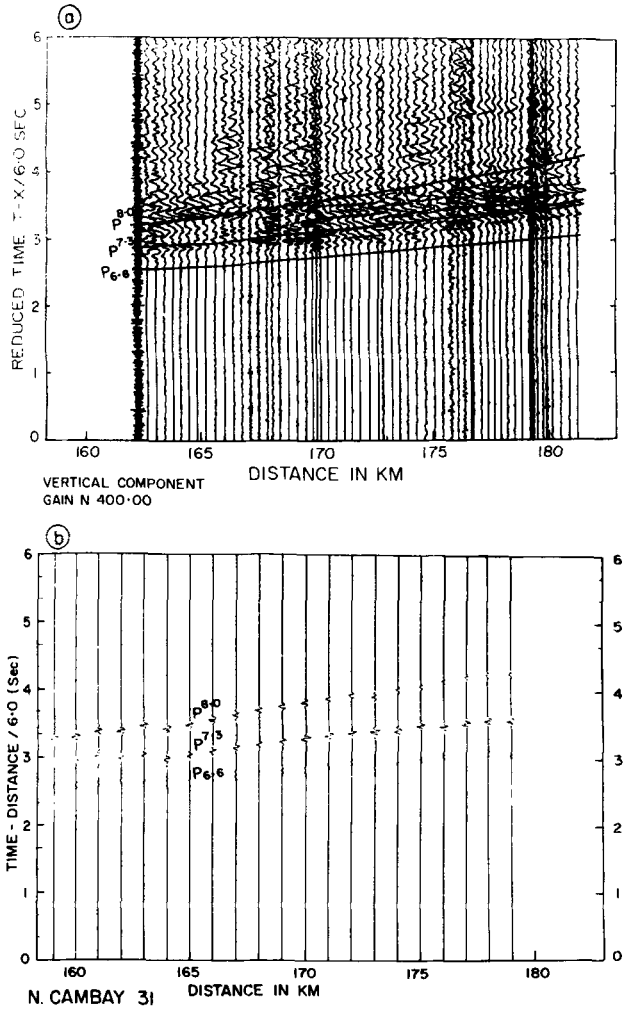

Figure 15. Record section of (a) observed and (b) ray synthetic seismograms on Line 3 for SP 31. The shot point is located at 70 km distance from right margin. Traveltime curves shown are calculated for various phases for the model shown in Fig. 16. In (a) the wide-angle reflections ($P^{7.3}$ and $P^{8.0}$) can be seen at 168–180 and 162–170 km respectively.

India and other associated regions were results of the rifting above a region of anomalously hot mantle around the Reunion plume. Dietz & Holden (1970) opined that the Deccan lava poured out following episodes of intense igneous intrusion that accompanied tectonic activities on the western margin of India when it crossed the mantle hotspot near the equator.

Hooper (1990), however, is of the view that in the Deccan the continental crust was not undergoing extension during the formation of main dykes which fed the lava eruption. The primary event in the formation of the major flood basalt province was the upwelling of a mantle plume and the subsequent crustal extension; rifting and decompression were a consequence of the initiation of the plume. The mantle plume produced voluminous melt beneath a thick, fast-moving continental plate which was not under significant extensional strain and the subsequent extension along the west coast of India appears to be, in part, a consequence of the new plume which generated its own type of volcanicity. The modest volume of intermediate magma with a strong alkaline component generated by crustal extension differs in physical style and composition from the initial voluminous plume-related tholeitic magma. Richards & Duncan (1989) preclude any extraordinary degree of asthenospheric heating during the Deccan eruption as the Indian subcontinent was moving very rapidly (12–18 cm yr^{-1}) over the Reunion hotspot at that time. They also favour a mantle plume initiation to be responsible for flood basalt eruption instead of continental rifting.

The Cambay is one of the three major marginal rift basins (Kutch, Cambay and Narmada) in the western platform of the Indian craton (Fig. 2), which developed sequentially from north to south, during India's drift after the break up of Gondwana land (Biswas 1982). The Kutch rifting took place in late Triassic/early Jurassic, Cambay rifting in early Cretaceous and Narmada rifting in late Cretaceous. The eruption of the Deccan volcanism, around 65 Ma coincides with the Cretaceous–Tertiary boundary (Subbarao 1988). The age of the Deccan basalts has been estimated as 69–64 Ma (Venkatesan, Pande & Gopalan 1986). Duncan &

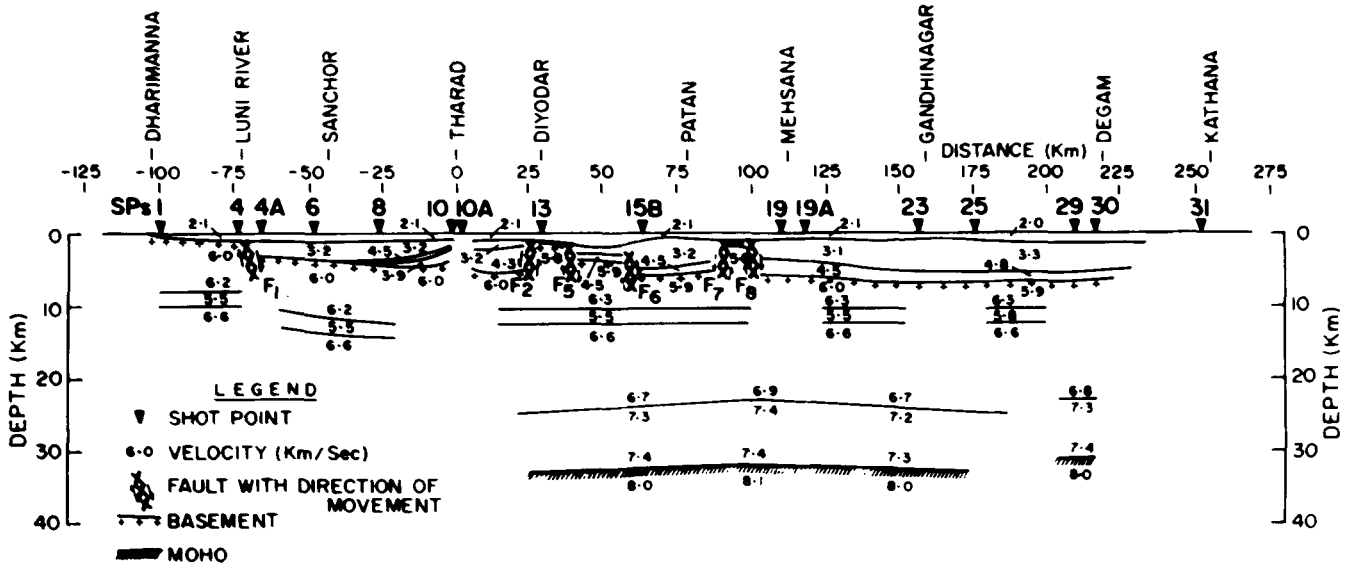

Figure 16. Crustal velocity model along North Cambay and Sanchor basins derived by modelling the refraction and wide-angle reflection data.

Pyle (1988) suggest a rapid eruption of Deccan Traps in perhaps 1 Myr, at 67.5 ± 0.3 Ma, at or very near to the Cretaceous–Tertiary boundary while Courtillot & Cisowski (1987) are of the opinion that the bulk of the Deccan Traps was extruded in only 0.5 Myr (main age 66 Ma). According to Pande *et al.* (1988), plugs and sheet-like bodies of alkali basalt coexist with tholeitic basalt in the Kutch region (near the Cambay basin) though a direct relationship cannot be established between the two. The age of the alkali basalts (64.4 ± 0.6 Ma to 67.7 ± 0.7 Ma) overlaps with those of the tholeitic basalts (66.8 ± 0.3 Ma) in this region.

It can, therefore, be established that at the time of Deccan Trap volcanism the Cambay was an existing rift system. The presence of a high-velocity (7.3 km s^{-1}) lower crustal layer above a relatively thin crust (31–33 km) as brought out by our studies, the presence of the Deccan Traps throughout the basin, and the mantle updoming in the Gulf of Cambay region with the associated high thermal anomaly (Biswas 1987) seem to favour the model proposed by White & McKenzie (1989) for volcanic eruption. This is further supported by more than 3200 m thick Traps in the Ankaleswar deep well (ONGC, personal communication; the well had to be terminated in the Traps at about 5700 m depth), about 120 km south of Cambay (Fig. 1). The information on the structure of the lithosphere in this region might provide further clues to solve the controversy regarding the origin of Deccan flood basalts.

Evidence that the subsidence of the rift continued during the Tertiaries is the large thickness of these sediments (maximum 4000 m) brought out by the present studies. A part of the subsidence was probably caused by reactivation of the western coast fault due to India–Asia collision during early Tertiary (Biswas 1987, 1988). High heat flow and prolific oil generating qualities of the early Tertiaries in this region suggest further subsidence due to relative thermal cycles associated with different rifting phases and mantle upwarp, during the Tertiaries.

The relatively thin crust (31–33 km) in the Cambay basin as compared to thicker crust (35–42 km) in the Saurashtra, across the Narmada lineament (Kaila *et al.* 1980, 1989) and the Koyna region (Krishna *et al.* 1989) suggests that the crustal thinning is related to various phases of mantle upwarp in the Cambay basin. The shallow Moho and the high-velocity lower crust, which will have higher density than the normal crust (White & McKenzie 1989), seem to have adequately compensated the gravity effect of the sedimentary thickness, thus giving rise to the observed Bouguer anomaly values (Fig. 4) within the Cambay basin. The upper crustal low-velocity zone brought out by the present studies may be due to the presence of free fluids released by metamorphic reactions at lower crustal levels (Percival & Barry 1987) or partial melting at the upper mantle depths (Raval 1989).

7 CONCLUSIONS

Based on the DSS studies in the north Cambay and Sanchor basins in western India, the following conclusions can be drawn.

(1) Four sedimentary sub-basins can be delineated: the north Sanchor basin, the south Sanchor basin, the Patan basin and Gandhinagar basin.

(2) The Deccan Traps form the basement of the Tertiary sediments. However, the Traps seem to be absent in the northern part of the Sanchor basin and are very thin in the Patan basin.

(3) The chances that Mesozoic sediments are present below the Deccan Traps are very small in the Patan basin, while in other sub-basins this is quite favourable.

(4) The maximum depth to the basement in the area of investigation is about 7700 m in the Gandhinagar basin.

(5) The maximum thickness of the upper crust is 15 km. The velocity in the sub-basement depths of the upper crust varies between 5.8 and 6.3 km s^{-1}.

(6) The bottom of the upper crust is marked by a low-velocity zone in which the velocity is about 5.5 km s^{-1}.

(7) The lower crustal thickness of about 20 km consists of two layers. In the upper layer the velocity is in the range of 6.6–6.9 km s^{-1}. At 21–23 km depth the velocity increases to 7.3 km s^{-1} and remains in the range of 7.3–7.4 km s^{-1} in the lower layer.

(8) The Moho discontinuity is at a rather shallow depth of 31–33 km in this region.

(9) The high-velocity lower crust indicates underplating of the crust due to mantle upwelling and rifting with large-scale extrusion of the Deccan Traps.

(10) The large thickness of Tertiary sediments and the shallow Moho within the Cambay basin indicate several stages of mantle upwarp and basin subsidence from the late Cretaceous to the Tertiary time.

ACKNOWLEDGMENTS

We are thankful to the Director, NGRI for kind permission to publish this paper. We are specially thankful to Dr Hooper for the preprint of his interesting article in *Nature*. Our thanks are also due to Messrs V. Sridhar, G. B. K. Shankar and G. Vidyasagar for their assistance in data processing and plotting the seismograms, and to Mr M. Shankaraiah for his help in drafting the figures. DSS studies in the north Cambay basin were financially sponsored by KDMIPE, ONGC, Dehradun. We thank the reviewers of this paper for their valuable comments.

REFERENCES

Biswas, S. K., 1982. Rift basins in western margins of India and their hydrocarbon prospects with special reference to Kutch basin, *Am. Assoc. Petrol. Geol.*, **66,** 1497–1513.

Biswas, S. K., 1987. Regional tectonic framework, structure and evolution of western marginal basins of India, *Tectonophysics*, **135,** 305–327.

Biswas, S. K., 1988. Structure of the western continental margins of India and related igneous activity, in *Deccan Flood Basalts*, vol. 10, pp. 371–390, ed. Subbarao, K. V., Mem. Geol. Soc. India, Bangalore.

Biswas, S. K. & Deshpande, S. V., 1983. Geology and hydrocarbon prospects of Kutch, Saurashtra and Narmada basin, *Petrol. Asia J.*, **6,** 111–126.

Červený, V. & Pšenčík, I., 1981. PROGRAM SEIS81: 2-Dimensional ray package, *Res. Rep. Inst. Geophys.*, Charles University, Prague.

Červený, V. & Pšenčík, I., 1983. PROGRAM SEIS83: Numerical modelling of seismic wave fields in 2-D laterally varying layered structures by the ray method, *Res. Rep. Inst. Geophys.*, Charles University, Prague.

Choubey, V. G., 1971. Narmada–Son lineament, India, *Nature*, **232**, 38–40.

Courtillot, V. E. & Cisowski, S., 1987. The Cretaceous–Tertiary boundary events, External or internal causes?, *EOS, Trans. Am. geophys. Un.* **68**, 193–200.

Dietz, R. S. & Holden, J. C., 1970. Reconstruction of Pangaea, breakup and dispersion of continents, Permian to present, *J. geophys. Res.*, **94**, 4939–4956.

Duncan, R. A. & Pyle, D. G., 1988. Rapid eruption of Deccan flood basalts, western India, in *Deccan Flood Basalts*, vol. 10, pp. 1–10, ed. Subbarao, K. V., Mem. Geol. Soc. India, Bangalore.

Geological Survey of India, 1962. *Geological Map of India*, 6th edn, Calcutta.

Hooper, P. R., 1990. The timing of crustal extension and the eruption of continental flood basalts, *Nature*, **345**, 246–249.

Kaila, K. L., Tewari, H. C. & Sarma, P. L. N., 1980. Crustal structure from deep seismic sounding studies along Navibandar–Amreli profile in Saurashtra, *Mem. Geol. Soc. India*, **3**, 218–232.

Kaila, K. L., Krishna, V. G. & Mall, D., 1981. Crustal structure along Mehmadabad–Billimora profile in the Cambay basin, India, from deep seismic soundings, *Tectonophysics*, **76**, 99–130.

Kaila, K. L., Rao, I. B. P., Koteswara Rao, P., Madhava Rao, N., Krishna, V. G. & Sridhar, A. R., 1989. DSS studies over Deccan Traps along the Thuadara–Sendhwa–Sindad profile across Narmada–Son lineament, India, in *Properties and Processes of the Earth's Lower Crust*, pp. 127–141, AGU Monogr. 51, IUGG 6, eds. Mereu, R. F., Mueller, St. & Fountain, D. M., Washington, DC.

Krishna, V. G., Kaila, K. L. & Reddy, P. R., 1989. Synthetic seismogram modelling of crustal seismic record sections from the Koyna DSS profiles in western India, in *Properties and Processes of the Earth's Lower Crust*, pp. 143–157, eds. Mereu, R. F., Mueller, St. & Fountain, D. M., AGU Monogr. 51, IUGG 6, Washington, DC.

National Geophysical Research Institute, 1978. *Gravity Map Series of India*, NGRI/GPH-2, Hyderabad.

Pande, K., Venkatesan, T. R., Gopalan, K., Krishnamurty, P. & Macdougall, J. D., 1988. $^{40}Ar/^{39}Ar$ ages of Alkali basalts from Kutch, Deccan volcanic province from India, in *Deccan Flood Basalts*, vol. 10, pp. 145–150, ed. Subbarao, K. V., Mem. Geol. Soc. India, Bangalore.

Pervical, J. A. & Barry, M. J., 1987. The lower crust of the continent, in *Composition, Structure and Dynamics of the Lithosphere–Asthenosphere System*, vol. 16, pp. 33–60, eds Fuchs, K. & Froidevaux, C., Geodynamics Series V, American Geophysical Union, Washington, DC.

Raju, A. T. R. & Srinivasan, S., 1983. More hydrocarbon from well explored Cambay basin, *Petrol. Asia J.*, **6**, 25–35.

Raval, U., 1989. On hotspots, Meso-Cenozoic tectonics, and possible thermal networking beneath the Indian continent, in *Advances in Geophysical Research in India*, pp. 314–330, Indian Geophysical Union, Hyderabad.

Richards, M. A. & Duncan, R. A., 1989. Flood basalts and plume initiation events: Active vs passive rifting, Abs. San Francisco meeting, Dec. 4–8, 1989, *EOS, Trans. Am. geophys. Un.*, 1357.

Scott, J. H., Tibbvetti, B. L. & Burdick, P. G., 1972. *Computer Analysis of Seismic Refraction Data*, US Department of Interior, Ref. No. 7595, Denver, CO.

Subbarao, K. V., 1988. Introduction to Deccan Flood basalts, *Mem. Geol. Soc. India*, **10**, 5–13.

Venkatesan, T. R., Pande, K. & Gopalan, K., 1986. $^{40}Ar/^{39}Ar$ dating of Deccan basalts, *J. Geol. Soc. India*, **27**, 102–109.

West, W. D., 1962. The line of the Narmada and Son valley, *Curr. Sci.*, **31**, 143–144.

White, R. S. & McKenzie, D. P., 1989. Magmatism at rift zones: The generation of volcanic continental margins and flood basalts, *J. geophys. Res.*, **94**, 7685–7729.